

A HYPER SUPRIME-CAM VIEW OF
THE INTERACTING GALAXIES OF THE M81 GROUP[†]SAKURAKO OKAMOTO¹, NOBUO ARIMOTO^{2,3}, ANNETTE M.N. FERGUSON⁴, EDOUARD J. BERNARD⁴, MIKE J. IRWIN⁵,
YOSHIHIKO YAMADA⁶, AND YOUSUKE UTSUMI⁷¹Shanghai Astronomical Observatory, Nandan road, Shanghai, 200030, China²Subaru Telescope, National Astronomical Observatory of Japan, 650 North A'ohoku Place Hilo, HI 96720, U.S.A.³The Graduate University for Advanced Studies, Osawa 2-21-1, Mitaka, Tokyo, 181-8588, Japan⁴Institute for Astronomy, University of Edinburgh, Royal Observatory, Blackford Hill, Edinburgh, EH9 3HJ U.K.⁵Institute of Astronomy, University of Cambridge, Madingley Road, Cambridge CB3 0HA, U.K.⁶National Astronomical Observatory of Japan, Osawa 2-21-1, Mitaka, Tokyo, 181-8588, Japan⁷Hiroshima Astrophysical Science Center, Hiroshima University, Kagamiyama 1-3-1, Higashi-Hiroshima, Hiroshima 739-8526, Japan*Draft version March 2, 2024*

ABSTRACT

We present the first results of a wide-field mapping survey of the M81 group conducted with Hyper Suprime-Cam on the Subaru Telescope. Our deep photometry reaches ~ 2 magnitudes below the tip of the red giant branch (RGB) and reveals the spatial distribution of both old and young stars over an area of $\sim 100 \times 115$ kpc at the distance of M81. The young stars ($\sim 30 - 160$ Myr old) closely follow the neutral hydrogen distribution and can be found in a stellar stream between M81 and NGC 3077 and in numerous outlying stellar associations, including the known concentrations of Arp's Loop, Holmberg IX, an arc in the halo of M82, BK3N, and the Garland. Many of these groupings do not have counterparts in the RGB maps, suggesting they may be genuinely young systems. Our survey also reveals for the first time the very extended ($\geq 2 \times R_{25}$) halos of RGB stars around M81, M82 and NGC 3077, as well as faint tidal streams that link these systems. The halos of M82 and NGC 3077 exhibit highly disturbed morphologies, presumably a consequence of the recent gravitational encounter and their ongoing disruption. While the halos of M81, NGC 3077 and the inner halo of M82 have the similar $(g-i)_0$ colors, the outer halo of M82 is significantly bluer indicating it is more metal-poor. Remarkably, our deep panoramic view of the M81 group demonstrates that the complexity long-known to be present in HI is equally matched in the low surface brightness stellar component.

Subject headings: galaxies: groups: individual (M81) — galaxies: halos — galaxies: individual (M81, M82, NGC 3077) — galaxies: interactions — galaxies: stellar content — galaxies: structure

1. INTRODUCTION

Over the last decade, deep studies of nearby galaxies have led to the discovery of vast stellar envelopes that are often rich in substructure (Mihos et al. 2005; Martínez-Delgado et al. 2010). These components are naturally predicted in models of hierarchical galaxy assembly and their observed properties place important constraints on the amount, nature and history of satellite accretion (e.g. Bullock & Johnston 2005; Pillepich et al. 2014). Due to their very low surface brightness, one of the most effective ways of mapping the peripheral regions of galaxies is through resolved star studies. For example, dedicated surveys of red giant branch (RGB) stars around M31 have revealed a stellar halo extending to more than ~ 200 kpc that is dominated by tidal debris features (e.g. Ibata et al. 2001; Ferguson et al. 2002; McConnachie et al. 2009; Ibata et al. 2014). Similarly, the Sloan Digital Sky Survey (SDSS) has been used to explore main-sequence (MS) turn off stars in the halo of the Milky Way, leading to many discoveries of new substructures, satellites and a refined characterization of halo and thick disk properties (e.g. Belokurov et al. 2007).

Using wide-field cameras equipped to 8m class telescopes, it has recently become possible to extend

these studies to systems beyond the Local Group (e.g. Mouhcine et al. 2010; Barker et al. 2012; Crnojević et al. 2013). Located at a distance of 3.6 Mpc (Freedman et al. 1994), M81, is a prime target for wide-field mapping of its resolved stellar content. Spectacular neutral hydrogen images have demonstrated the significant tidal interactions between M81 and its two brightest neighbors, M82 and NGC 3077, which modelling suggests have taken place in the last 300 Myrs (e.g. van der Hulst 1979; Yun et al. 1994; Yun 1999; Chynoweth et al. 2008). Deep photometry from the Hubble Space Telescope (HST) has been used to argue that the outlying HI concentrations Arp's Loop (AL), and Holmberg IX (HoIX) may be tidal dwarf galaxies formed as a result of these interactions (Makarova et al. 2002; de Mello et al. 2008; Sabbi et al. 2008). In NGC 3077, 90% of the atomic hydrogen is located eastward of the center, in the tidal arm called “the Garland” where young stars have been observed (Karachentsev et al. 1985; Sakai & Madore 2001; Weisz et al. 2008). Several other young star concentrations have been associated with peaks in the HI gas (Durrell et al. 2004; Sun et al. 2005; Davidge 2008b; Mouhcine & Ibata 2009; Chiboucas et al. 2013), however, the global properties of this population throughout the M81 group are still poorly known.

The old stellar content around M81 has also been studied using large telescopes. Barker et al. (2009) found

[†] Based on data collected at Subaru Telescope, which is operated by the National Astronomical Observatory of Japan.

the evidence for a faint, extended structural component beyond the bright optical disk of M81 from wide-field images taken by Subaru/Suprime-Cam. They detected no colour gradient in this structure out to 44 kpc; Monachesi et al. (2013) used HST pointings to extend this result to 50 kpc. Chiboucas et al. (2013) confirmed 12 new dwarf satellites as members of the M81 group, discovered from a 65 deg² survey with CFHT/MegaCam.

In this paper, we present the first results from a deep wide-field imaging survey of the M81 group that we are conducting with the new prime-focus imager, Hyper Suprime-Cam (HSC), on the Subaru Telescope. We report on the analysis of the inner 4 deg² area, corresponding to a region spanning 100 × 115 kpc at the distance of the galaxy, which reveals the first truly panoramic view of the low surface brightness stellar component. The observations and data reduction are described in Section 2. Section 3 and 4 present our analysis and results, which are discussed and conclusions drawn in Section 5.

For this paper, we adopt a distance modulus for M81 and associated systems of $(m - M)_0 = 27.79$ (Radburn-Smith et al. 2011), position angles for M81, M82, and NGC 3077 of 157°, 67.5°, and 55.0° east of north, R_{25} radii for M81, M82, NGC 3077 and HoIX of 13.8', 5.6', 2.7' and 2.5', respectively (de Vaucouleurs et al. 1991; Karachentsev et al. 2004).

2. OBSERVATIONS AND DATA REDUCTION

We observed the central region of the M81 group in the g - and i -bands using 4 pointings of Subaru/HSC during the nights of January 21 and 22, 2015 (PI: S. Okamoto; Proposal ID: S14B-101) with the seeing ranged from 0.6'' to 0.9''. The HSC consists of 104 CCD detectors and provides a field-of-view of 1.76 deg² with a pixel scale of 0.17'' (Miyazaki et al. 2012). The observations were obtained as part of a survey to map the M81 group with 7 HSC pointings. In this paper, we focus on the inner 4 deg² of our survey which overlaps the SDSS footprint (York et al. 2000).

The raw images were processed using the HSC pipeline (version 3.2.2), which is based on a software suite being developed for the Large Synoptic Survey Telescope (LSST) project (Ivezic et al. 2008; Axelrod et al. 2010). For the processed images, the DAOPHOT in IRAF was used to obtain the PSF photometry of resolved stars (Stetson 1987). Astrometric and photometric calibrations were done using the SDSS catalog. Artificial star tests were performed on some parts of the reduced images using the ADDSTAR in DAOPHOT, and indicate that our photometry is at least 50% complete to 26 mag in both bands, except for the inner regions of galaxies. We separate point sources from extended sources in the same manner as for Suprime-Cam images in Okamoto et al. (2012). Full details of the observations and data reduction will be presented in a forthcoming paper.

3. THE COLOR-MAGNITUDE DIAGRAMS

Figure 1 shows the resulting CMD of roughly 550,000 point sources found in the whole 4 deg² field. The error bars represent the photometric errors at $(g - i)_0 = 0$, as estimated by the artificial star tests. The Galactic extinction is taken from Schlafly & Finkbeiner (2011). Since the extinction varies across the observed field, we

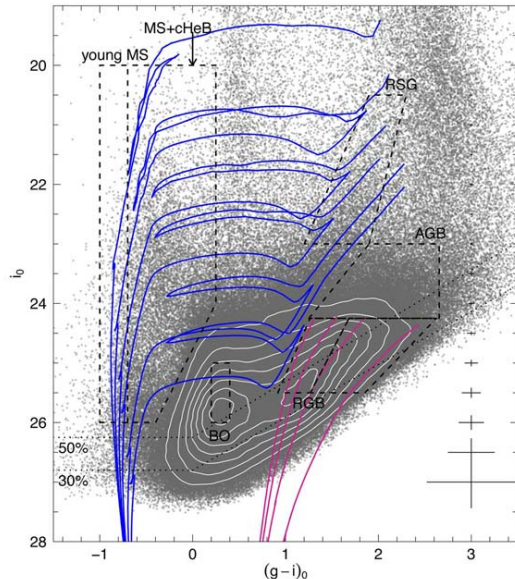


FIG. 1.— Dereddened CMD of stellar objects located within the central 4 deg² area. The dashed boxes delineate the selection criteria for different stellar populations and are used to construct the maps presented in Figure 3. Theoretical Padova isochrones, adjusted at $(m - M)_0 = 27.79$, are shown for a 12 Gyr old population with $[M/H] = -2.2, -1.75, -1.3, -0.75$ from the left to the right (magenta), and for a $[M/H] = -0.75$ population with ages of 10, 18, 32, 50, 100, 160 Myr from top to bottom (blue). The dotted lines represent the completeness levels of 50% and 30%.

apply a reddening correction to each source individually according to its location, assuming a Fitzpatrick (1999) reddening law with $R_V = 3.1$. The central region within $r = 15'$ of M82 in the reddening map shows significantly higher extinction $E(B - V) \sim 0.16$ that includes the internal reddening of M82. Therefore, we replace it with $E(B - V) = 0.075$.

To aid in understanding the range of stellar populations present, theoretical Padova isochrones are overlaid (Bressan et al. 2012). We find that tracks with metallicity $[M/H]$ varying from ~ 0.0 to below -1.0 for young stars, and $[M/H] \lesssim -1.0$ for old stars provide a good description of the data, in agreement with other studies of smaller regions (Makarova et al. 2002; Williams et al. 2009; Durrell et al. 2010; Kudritzki et al. 2012; Barker et al. 2009; Monachesi et al. 2013). We use $[M/H] = -0.75$ as the fiducial value for the young population, and overlay the 10-160 Myr old isochrones as blue solid lines in Figure 1. For the old population, we plot $[M/H] = -2.2$ to -0.75 isochrones of 12 Gyr old as magenta solid lines.

Figure 1 is mostly populated by old RGB stars located at $i_0 \gtrsim 24$ and $(g - i)_0 \sim 1.2$. As discussed by Barker et al. (2009), the over-density at $i_0 \sim 26$ and $(g - i)_0 \sim 0.3$ (labelled BO for ‘blue objects’) mostly samples unresolved background sources. On the blue side of the foreground Galactic dwarf sequence (at $(g - i)_0 \sim 0.4$), young MS and core Helium burning (cHeB) stars in the M81 group are found. We select stars in different evolutionary phases as shown by the dashed boxes in Figure 1: MS, cHeB, Red Supergiant (RSG), Asymptotic Giant Branch (AGB) and RGB stars. The boundaries were adopted to limit the number of foreground/background

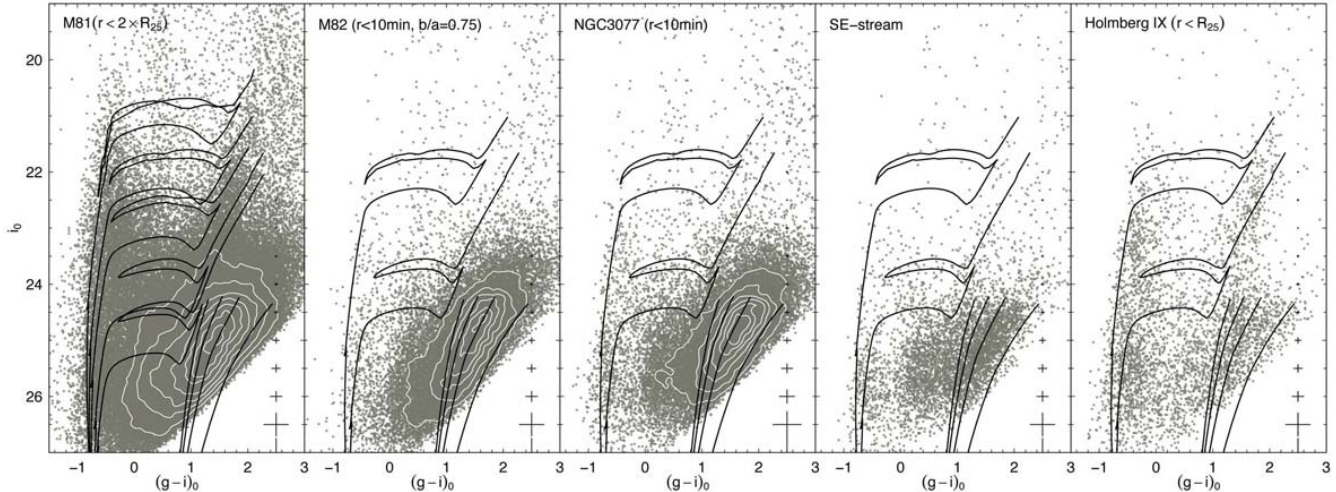


FIG. 2.— Dereddened CMDs of stellar sources in the disk and halo (see text) of each galaxy, and in the SE-stream. The overplotted isochrones are the same as those in Figure 1.

contaminants. The young MS box mainly contains stars younger than ~ 50 Myr old while the MS+cHeB box is occupied by MS and post MS stars of < 100 Myr old. On the red bright side, the polygon contains RSGs about 25-160 Myr old with some contamination from Galactic disk stars. Above the RGB tip at $i_0 = 24.25$, intermediate age (~ 0.5 -8 Gyr) AGBs are found (Marigo et al. 2008). From the RGB tip to about 1.5 magnitude below, the blue and red RGBs boxes contain stars older than 1 Gyr. We also examine the spatial distribution of BO sources. We note that the completeness of our photometry decreases towards the red, as shown by the dashed lines, so our RGB sample may be biased toward the bluer side.

Figure 2 shows the dereddened CMDs of the disk and halo of each galaxy, HoIX and the stream between M81 and NGC 3077 (hereafter the SE-stream). Stars within $r = 2 \times R_{25}$ (i.e. $27.6'$ or 29 kpc) of M81, and within $10'$ (10.5 kpc) for M82 and NGC 3077, within $r = R_{25}$ ($2.5'$ or 2.6 kpc) of HoIX are shown (see dashed lines in Figure 3); an axis ratio of 0.75 has been used for M82 to take into account the varying flattening of the stellar distribution in the outer regions. We also select a $15' \times 6'$ area for the SE-stream between M81 and NGC 3077. Young blue MS and RSG can be easily seen in the M81 CMD, as well as vast numbers of RGBs. In M82 and NGC 3077, RGBs are prominent and some MSs exist, but few if any RSGs can be seen. We note that the area within R_{25} of each galaxy could not be resolved due to crowding, so we miss the stars of the M81 and M82 disks, and in NGC 3077 center. In the SE-stream, the most luminous MSs correspond to ~ 32 Myr old. In HoIX, several MSs, cHeBs and RSGs exist. Although we cannot resolve RGBs at the innermost ($< 1'$) of HoIX, the number density of RGBs in HoIX are comparable to those of other regions at the same distance from M81. Therefore, as discussed by Sabbi et al. (2008) with deeper HST images, most of the old component at HoIX may belong to M81 halo.

4. THE SPATIAL DISTRIBUTIONS OF YOUNG AND OLD COMPONENTS

Figure 3 shows the spatial distributions of HI gas (Yun et al. 1994), MS, cHeB, RSG, AGB, blue and red RGB stars, and BOs defined in Figure 1, without correction for the completeness and contaminants. In the upper panels, the solid ellipses represent the R_{25} radii of the three main galaxies.

The distribution of the young populations traced by the young MS, MS+cHeB and RSG stars agrees extremely well with that of the HI distribution, except for the stream at the northwest of NGC 3077 where few stars are seen. The young MSs are mainly concentrated in the spiral arms of M81, at the north-west side (hereafter NW-arm), AL, HoIX, BK3N, the Garland, and SE-stream. A number of small clumps are also seen as they follow HI blobs around these systems. The stellar concentration in the NW-arm was identified by Davidge (2008b) and was suggested to be part of the M81 arm by Barker et al. (2009). We confirm that it is connected to the stellar concentration on the north arm. The higher density regions in the SE-stream have been reported either as clumps or as a dwarf galaxy (d0959+68) in previous studies (Durrell et al. 2004; Mouhcine & Ibatá 2009; Chiboucas et al. 2013). As Chiboucas et al. (2013) discussed, these over-densities are clearly parts of a single stream. Near NGC 3077, many MSs are found in the Garland and up to about 8 kpc to the south and 10 kpc to the east where HI gas and dust emission have been observed (Walter et al. 2011). In M82, a prominent stellar feature can be seen at $(\Delta\alpha, \Delta\delta) \sim (0.1, 0.6)$, identified as an arc by Sun et al. (2005) and Davidge (2008a). MSs are also distributed well beyond the R_{25} radius up to the projected distance of about 16 kpc from M82.

Stars in the MS+cHeB box have a very similar distribution to that of the young MSs. The arc at the southeast of M82 appears to have a clumpy shape, but it is an artificial appearance due to the overlap of plotted points (see Figure 5). Interestingly, our maps show that there is another young stellar feature on the opposite side of M82 that appears to be aligned with the southern arc and may therefore be related. The selection box of MS+cHeB stars includes some contamination, mainly

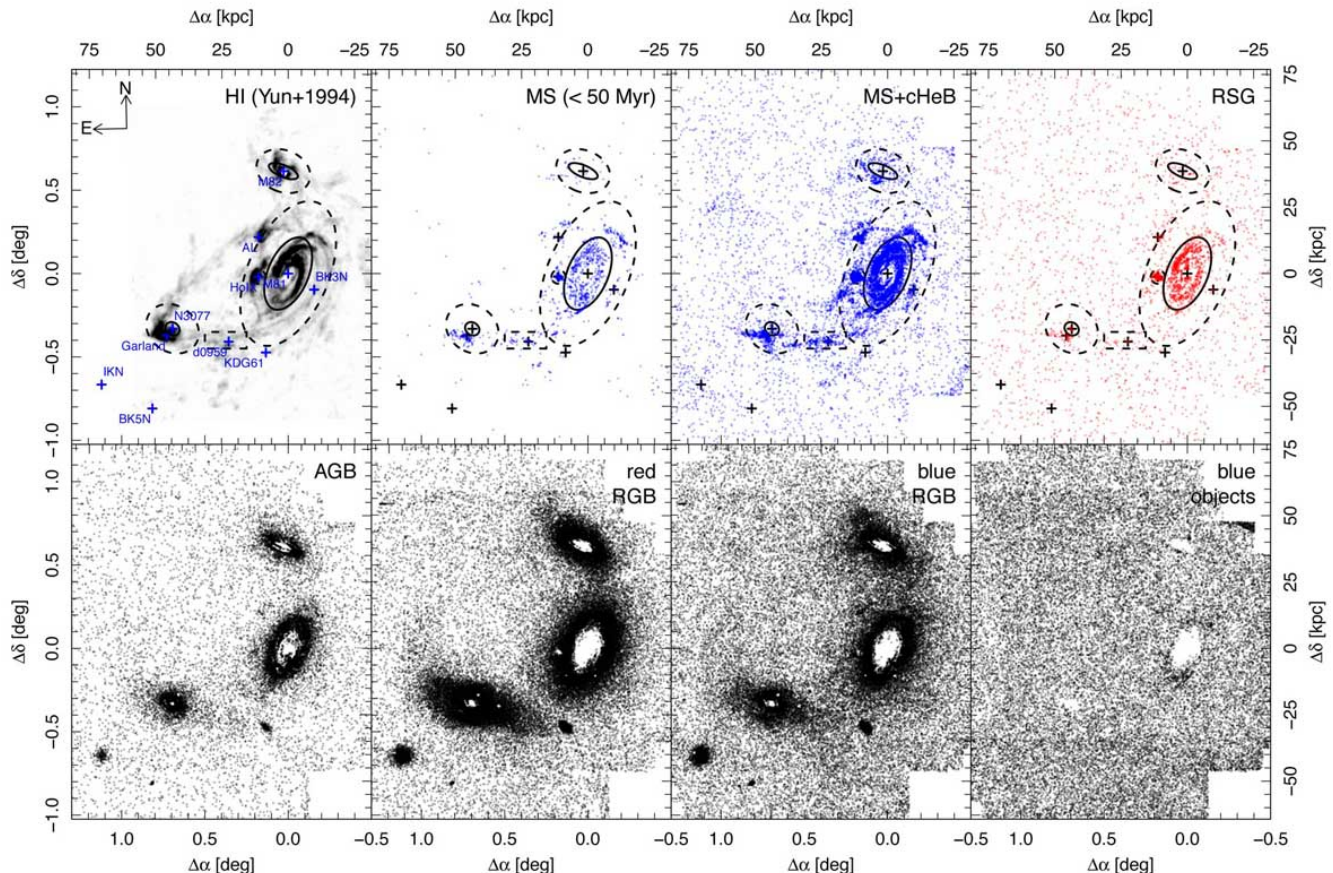


FIG. 3.— The spatial distribution of stars in each evolutionary phase selected in Figure 1. Shown from the top left to the bottom right are the HI column density map taken from Yun et al. (1994), the spatial distributions of stars in evolutionary phases and blue contaminants. The cross marks represent the centers of known M81 group members. The solid lines are R_{25} of galaxies, with axis ratios of M82 and NGC 3077 of $b/a = 0.38$ and 0.83 , and an inclination angle of $i = 58^\circ$ for M81, respectively. The dashed lines outline the regions used for the CMDs in Figure 2.

from background blue objects, as can be seen by the low-level uniform distribution of sources through out the area. In the top-right panel of Figure 3, the distribution of the RSGs is almost the same as that of MSs and cHeBs. However, the fainter substructures – SE-stream, M82-arc, some clumps around HoIX and AL, and BK3N – can not be seen in this map due to the shorter lifetime and the lower number of RSGs compared to MSs.

In contrast, the older populations (AGB, RGBs) have a much smoother distribution than the younger stars. Old stars are mainly embedded in the halos which reach far beyond the R_{25} radii of three galaxies. The sizes of these RGB halos are considerable, and they may even overlap (see Figure 4). While the M82 halo seems to be more extended in the blue RGB map, the halos of M81 and NGC 3077 are more prominent in the red RGB map, suggesting they have a higher mean metallicity. In the contour map of red RGBs in Figure 4, a tidal stream between M81 and M82 can clearly be seen, and the outer regions of M82 and NGC 3077 exhibit an “S-shaped” morphology. The dwarf galaxies IKN, BK5N, and KDG61 cannot be seen in the maps of young stars, but appear as over-densities of old populations, implying they have not formed as a result of the recent interaction.

In the bottom-right panel of Figure 3, we plot the dis-

tribution of BOs at $25 < i_0 < 26$ and $0.2 < (g-i)_0 < 0.4$. The uniform distribution of these sources supports their identification as contaminants, since the star/galaxy separation in our photometry degrades at magnitude fainter than about 24 mag in both g - and i -bands.

5. DISCUSSION AND SUMMARY

We find that the young intra-group population in the M81 group traces the filamentary structures of the HI gas connecting M81, M82, and NGC 3077, confirming the results of several smaller field-of-view studies. The left panel of Figure 5 shows the spatial distribution of stars in young MS and MS+cHeB boxes of Figure 1, which are color coded according to i -band magnitude in a transparent manner, so that colors of overlapping points represent the average color. Bright stars are mainly located in the inner disk of M81, while most of young stars in AL, NW-arm, BK3N, Garland, and other debris features are fainter than $i_0 \sim 24$ and have similar luminosity distributions to the SE-stream, implying ages of 30-160 Myr old. This suggests that star formation in these tidal features was synchronized, and may have stopped about 30 Myrs ago. The SE-stream is slightly inclined from the southeast to the northwest, whereas the tail of RGB stars in NGC 3077 at the same location is extended to-

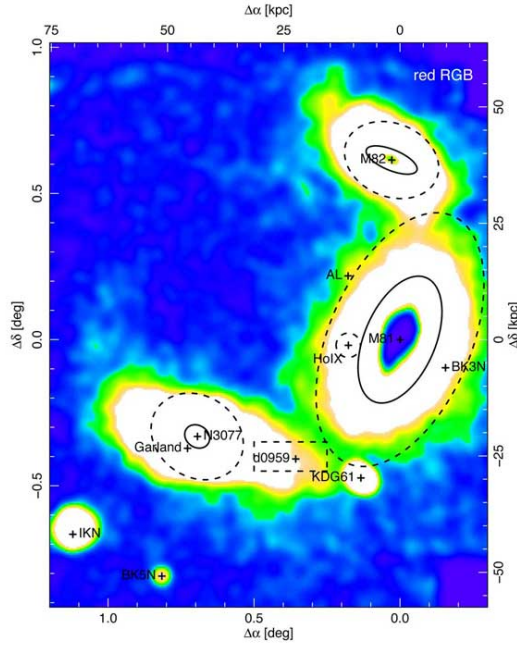


FIG. 4.— The isodensity contour map of red RGB stars, featured to faint structures up to 20σ above the background level. The kernel density is estimated with the bandwidth of $1.2'$. The marks and lines are the same as in Figure 3.

ward the northeast-southwest. That fact that these spatial distributions do not exactly match may indicate that the SE-stream comes from material torn from M81 while the RGB tail is material stripped from NGC 3077. The color of HoIX is slightly greener than other clumps and streams, meaning it includes some bright (younger) MS stars as we see in Figure 2.

The right panel of Figure 5 shows the color distribution of RGBs, which can be interpreted as a rough proxy for metallicity. The bluest (index=0) and reddest (index=1) colors correspond to $[M/H] = -2.3$ and -0.75 , respectively, assuming 12 Gyr old age. The RGBs between the solid and dashed lines of M81, M82 and NGC 3077 have the similar colors; the medians of the color indexes are 0.41, 0.40, 0.46 respectively, corresponding to $[M/H] \sim -1.4$, -1.4 and -1.3 . This M81 halo metallicity is slightly lower than the value of $[M/H] \sim -1.1$ derived from previous Subaru imagery and the estimation $[Fe/H] = -1.2$ from deep HST photometry (Barker et al. 2009; Monachesi et al. 2013). This might be due to the missing metal-rich RGB stars in our photometry, since the completeness gets worse at redder colors. The halo of M82 has a color gradient from the inner greener area to the outer bluer region; the greener part is also extended toward the northeast and along the direction of

the young stellar arc. Note that we do not correct for the internal extinction of each galaxy, so it is not possible from this study alone to determine if these are the bona fide features of the M82 halo. The tidal stream between M81 and M82 is also predominantly blue in color, indicating that this is material being stripped from M82 onto M81.

In Figure 4 and 5, the NGC 3077 halo is extended far beyond the R_{25} , and has a rhombus shape stretched in the east-west direction. In the outermost region, an S-shape distortion can be discerned, which is similar to what was found around M33 (McConnachie et al. 2010). The component in the northwest appears to reach a maximum projected radius from NGC 3077 of ~ 65 kpc, but does not appear to trace the HI distribution in this region. The S-shaped structure is typical of an interacting dwarf galaxy with a larger companion (e.g. Peñarrubia et al. 2009). Numerical modelling suggests the encounters between NGC 3077, M81 and M82 took place ~ 200 -300 Myr ago (Yun 1999), which may not leave enough time to restore equilibrium in the NGC 3077 halo. We will return to the topic of the stellar streams in the M81 group in a later paper.

The close encounters between M81, M82 and NGC 3077 induced star formation in tidally stripped gas. As a consequence, new stellar concentrations were born out of these HI rich clumps, many of which lie far from the main bodies of the galaxies. Of these concentrations, only AL appears to have a clear counterpart in the RGB map. The presence of an older stellar component suggests that this object, like the dwarf galaxies IKN, BK5N, and KDG 61, may not have a tidal origin. The gravitational interactions between the M81 group galaxies have also significantly perturbed their older stellar components leading to disturbed halo morphologies and giant stellar streams which appear to connect all three systems. When combined with our forthcoming HSC observations of the west side of M81, these data will allow us to determine the true extent and nature of the intra-group debris and map the halos of the M81 group galaxies to unprecedented distances.

We are grateful to the entire staff at Subaru Telescope and the HSC team. We acknowledge the importance of Maunakea within the indigenous Hawaiian community. This paper makes use of software developed for the LSST. We thank the LSST Project for making their code available as free software at <http://dm.lsstcorp.org>. SO acknowledges support from the CAS PIFI scheme. AMNF and EJB acknowledge support from an STFC Consolidated Grant. This work was supported by the grants of CAS (XDB09010100), NSFC (11333003), and JSPS (Grant-in-Aid for Young Scientists B, 26800103).

REFERENCES

- Axelrod, T., Kantor, J., Lupton, R. H., & Pierfederici, F. 2010, in Society of Photo-Optical Instrumentation Engineers (SPIE) Conference Series, Vol. 7740, Society of Photo-Optical Instrumentation Engineers (SPIE) Conference Series, 15
- Barker, M. K., Ferguson, A. M. N., Irwin, M., Arimoto, N., & Jablonka, P. 2009, *AJ*, 138, 1469
- Barker, M. K., Ferguson, A. M. N., Irwin, M. J., Arimoto, N., & Jablonka, P. 2012, *MNRAS*, 419, 1489
- Belokurov, V., Zucker, D. B., Evans, N. W., et al. 2007, *ApJ*, 654, 897
- Bressan, A., Marigo, P., Girardi, L., et al. 2012, *MNRAS*, 427, 127
- Bullock, J. S., & Johnston, K. V. 2005, *ApJ*, 635, 931
- Chiboucas, K., Jacobs, B. A., Tully, R. B., & Karachentsev, I. D. 2013, *AJ*, 146, 126
- Chynoweth, K. M., Langston, G. I., Yun, M. S., et al. 2008, *AJ*, 135, 1983
- Crnojević, D., Ferguson, A. M. N., Irwin, M. J., et al. 2013, *MNRAS*, 432, 832
- Davidge, T. J. 2008a, *ApJ*, 678, L85
- . 2008b, *PASP*, 120, 1145

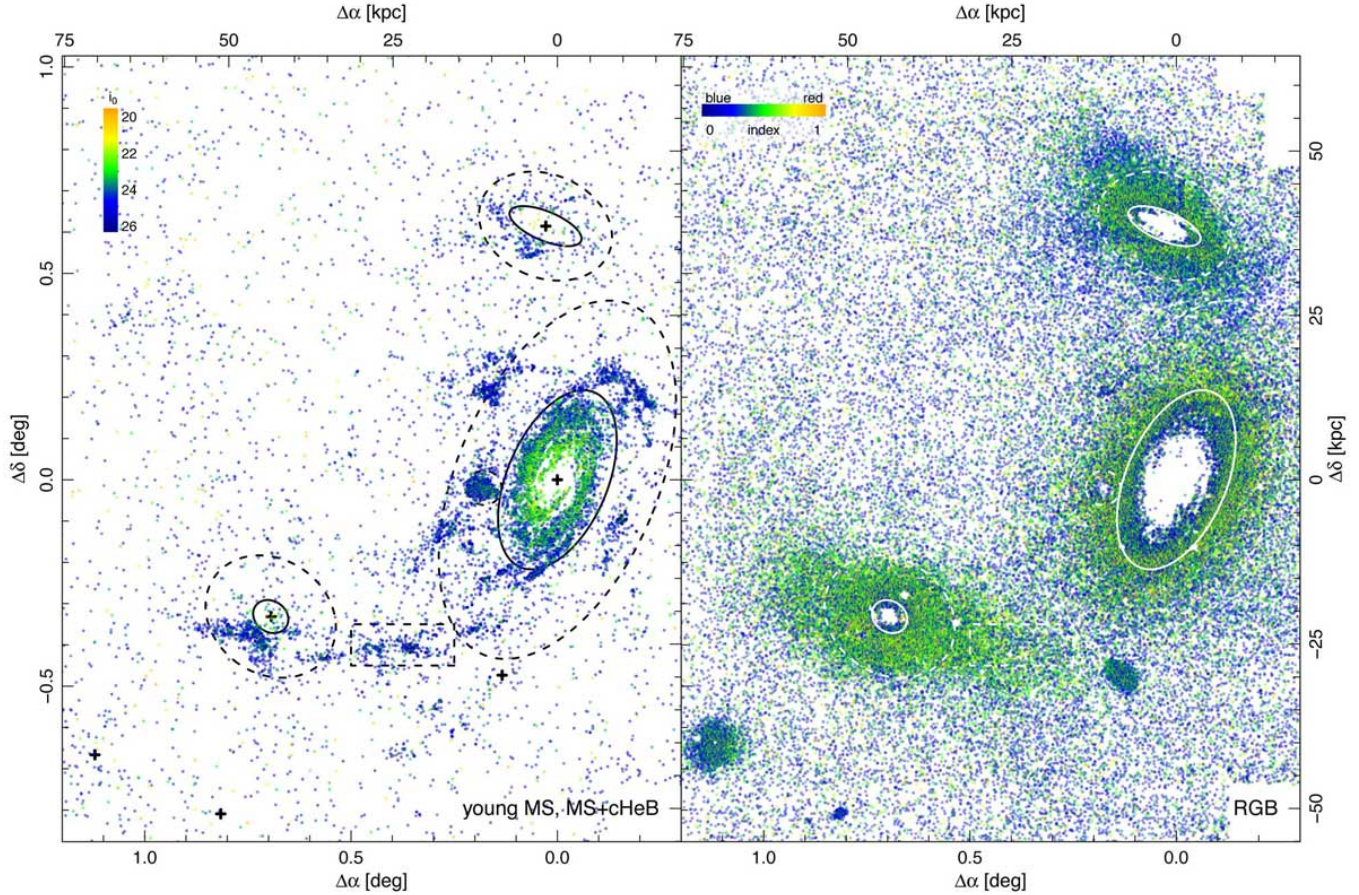


FIG. 5.— *Left*: The spatial distribution of MS and cHeB stars that are color coded according to the luminosity with transparency. *Right*: The spatial distribution of RGB stars. The color of each point represents the $(g-i)_0$ color of star with transparency. The marks and lines are the same as in Figure 3.

de Mello, D. F., Smith, L. J., Sabbi, E., et al. 2008, *AJ*, 135, 548
 de Vaucouleurs, G., de Vaucouleurs, A., Corwin, Jr., H. G., et al. 1991, *Third Reference Catalogue of Bright Galaxies. Volume I: Explanations and references. Volume II: Data for galaxies between 0^h and 12^h . Volume III: Data for galaxies between 12^h and 24^h .*
 Durrell, P. R., Decesar, M. E., Ciardullo, R., Hurley-Keller, D., & Feldmeier, J. J. 2004, in *IAU Symposium, Vol. 217, Recycling Intergalactic and Interstellar Matter*, ed. P.-A. Duc, J. Braine, & E. Brinks, 90
 Durrell, P. R., Sarajedini, A., & Chandar, R. 2010, *ApJ*, 718, 1118
 Ferguson, A. M. N., Irwin, M. J., Ibata, R. A., Lewis, G. F., & Tanvir, N. R. 2002, *AJ*, 124, 1452
 Fitzpatrick, E. L. 1999, *PASP*, 111, 63
 Freedman, W. L., Hughes, S. M., Madore, B. F., et al. 1994, *ApJ*, 427, 628
 Ibata, R., Irwin, M., Lewis, G., Ferguson, A. M. N., & Tanvir, N. 2001, *Nature*, 412, 49
 Ibata, R. A., Lewis, G. F., McConnachie, A. W., et al. 2014, *ApJ*, 780, 128
 Ivezić, Z., Tyson, J. A., Abel, B., et al. 2008, *ArXiv e-prints*, arXiv:0805.2366
 Karachentsev, I. D., Karachentseva, V. E., & Boerngen, F. 1985, *MNRAS*, 217, 731
 Karachentsev, I. D., Karachentseva, V. E., Huchtmeier, W. K., & Makarov, D. I. 2004, *AJ*, 127, 2031
 Kudritzki, R.-P., Urbaneja, M. A., Gazak, Z., et al. 2012, *ApJ*, 747, 15
 Makarova, L. N., Grebel, E. K., Karachentsev, I. D., et al. 2002, *A&A*, 396, 473
 Marigo, P., Girardi, L., Bressan, A., et al. 2008, *A&A*, 482, 883
 Martínez-Delgado, D., Gabany, R. J., Crawford, K., et al. 2010, *AJ*, 140, 962
 McConnachie, A. W., Ferguson, A. M. N., Irwin, M. J., et al. 2010, *ApJ*, 723, 1038

McConnachie, A. W., Irwin, M. J., Ibata, R. A., et al. 2009, *Nature*, 461, 66
 Mihos, J. C., Harding, P., Feldmeier, J., & Morrison, H. 2005, *ApJ*, 631, L41
 Miyazaki, S., Komiyama, Y., Nakaya, H., et al. 2012, in *Society of Photo-Optical Instrumentation Engineers (SPIE) Conference Series, Vol. 8446, Society of Photo-Optical Instrumentation Engineers (SPIE) Conference Series*, 0
 Monachesi, A., Bell, E. F., Radburn-Smith, D. J., et al. 2013, *ApJ*, 766, 106
 Mouhcine, M., & Ibata, R. 2009, *MNRAS*, 399, 737
 Mouhcine, M., Ibata, R., & Rejkuba, M. 2010, *ApJ*, 714, L12
 Okamoto, S., Arimoto, N., Yamada, Y., & Onodera, M. 2012, *ApJ*, 744, 96
 Peñarrubia, J., Navarro, J. F., McConnachie, A. W., & Martin, N. F. 2009, *ApJ*, 698, 222
 Pillepich, A., Vogelsberger, M., Deason, A., et al. 2014, *MNRAS*, 444, 237
 Radburn-Smith, D. J., de Jong, R. S., Seth, A. C., et al. 2011, *ApJS*, 195, 18
 Sabbi, E., Gallagher, J. S., Smith, L. J., de Mello, D. F., & Mountain, M. 2008, *ApJ*, 676, L113
 Sakai, S., & Madore, B. F. 2001, *ApJ*, 555, 280
 Schlafly, E. F., & Finkbeiner, D. P. 2011, *ApJ*, 737, 103
 Stetson, P. B. 1987, *PASP*, 99, 191
 Sun, W.-H., Zhou, X., Chen, W.-P., et al. 2005, *ApJ*, 630, L133
 van der Hulst, J. M. 1979, *A&A*, 75, 97
 Walter, F., Sandstrom, K., Aniano, G., et al. 2011, *ApJ*, 726, L11
 Weisz, D. R., Skillman, E. D., Cannon, J. M., et al. 2008, *ApJ*, 689, 160
 Williams, B. F., Dalcanton, J. J., Seth, A. C., et al. 2009, *AJ*, 137, 419
 York, D. G., Adelman, J., Anderson, Jr., J. E., et al. 2000, *AJ*, 120, 1579

Yun, M. S. 1999, in IAU Symposium, Vol. 186, Galaxy
Interactions at Low and High Redshift, ed. J. E. Barnes &
D. B. Sanders, 81

Yun, M. S., Ho, P. T. P., & Lo, K. Y. 1994, *Nature*, 372, 530